Single-particle probing of edge-state formation in a graphene nanoribbon

K. L. Chiu,[1] M. R. Connolly,[1,2] A. Cresti,[3] C. Chua,[1] S. J. Chorley,[1] F. Sfigakis,[1] S. Milana,[4] A. C. Ferrari,[4] J. P. Griffiths,[1] G. A. C. Jones,[1] and C. G. Smith[1]

[1]*Cavendish Laboratory, Department of Physics, University of Cambridge, Cambridge CB3 0HE, United Kingdom*

[2]*National Physical Laboratory, Hampton Road, Teddington TW11 0LW, United Kingdom*

[3]*IMEP-LAHC (UMR CNRS/INPG/UJF 5130), Grenoble INP Minatec, 3 Parvis Louis Néel, BP 257, F-38016 Grenoble, France*

[4]*Department of Engineering, University of Cambridge, Cambridge CB3 OFA, United Kingdom*

(Received 15 December 2011; revised manuscript received 12 April 2012; published 29 May 2012)

We investigate the effect of a perpendicular magnetic field on the single-particle charging spectrum of a graphene quantum dot embedded inline with a nanoribbon. We observe uniform shifts in the single-particle spectrum which coincide with peaks in the magnetoconductance, implicating Landau level condensation and edge state formation as the mechanism underlying magnetic field-enhanced transmission through graphene nanostructures. The experimentally determined ratio of bulk to edge states is supported by single-particle band-structure simulations, while a fourfold beating of the Coulomb blockade transmission amplitude points to many-body interaction effects during Landau level condensation of the $\nu = 0$ state.

DOI: 10.1103/PhysRevB.85.205452 PACS number(s): 73.63.Kv, 73.43.−f, 73.23.Hk

Graphene nanoribbons (GNRs) attract considerable attention due to their customizable electronic properties and compatability with existing semiconductor device processing. Unlike large-area graphene field-effect devices, at low temperature GNRs exhibit a length- and width-dependent transport gap where the conductance is suppressed for a range of source-drain bias voltages around the charge neutrality point.[1–8] Conduction in GNRs is widely believed to occur by hopping between localized and Coulomb-blockaded states, which form along the GNR due to edge roughness and potential disorder.[4,7,9–12] Within this framework the source-drain gap is not a band gap due to quantum confinement, but the Coulomb gap E_c of the domain dominating transport, while the transport gap includes the range of Fermi level where transport is dominated by both localized states and quantum confinement.[3]

In a perpendicular magnetic field, GNRs show a large positive magnetoconductance due to the suppression of both the transport and source-drain gaps.[13,14] Drawing from similar behavior in strongly disordered quasi-one-dimensional GaAs channels,[15,16] this effect has been attributed to an increase in the size ξ of the localized domains and the consequent decrease in the activation energy E_a required to hop between them.[14] The correlation between the Coulomb energy gap E_c and E_a in a magnetic field supports this picture.[12] One mechanism proposed for the increase in ξ is the elimination of coherent backscattering,[16] although the possibility that some role is also played by the formation of chiral magnetic edge channels has not been excluded.[12,14] Understanding this role has been hindered by the near absence of clear quantum Hall effects in GNRs at low magnetic fields (<10 T), but recent experiments performed at higher magnetic fields ($10 < B < 60$ T) have shown that quantized plateaus in the two-terminal conductance at filling factors $\nu = 2,6,10,\ldots$ are fully recovered when the magnetic length is less than the width W of the GNR.[17,18] This reopens the question as to whether the increase in ξ at a low field regime is also explicable in terms of partially scattered magnetic edge channels. So far this question has not been fully explored because the effects of Landau level condensation on the single-particle spectrum of individual localized states has not been observed and correlated with quantum Hall effects in the same device. In this work we investigate a GNR with an embedded quantum dot (QD) whose quasi-two-dimensional nature promotes the coexistence of strong localization with well developed oscillations in the magnetoconductance, even at a low magnetic field. By tracking the single-particle addition energy and transmission amplitude of the QD as a function of the magnetic field during these oscillations, we show they arise during Landau level condensation when the single particle states are delocalized in edge states. This suggests that edge channel formation also contributes to the increase in ξ observed in GNRs at a low magnetic field.

Our GNR is formed from a graphene flake mechanically exfoliated from natural graphite onto a highly doped Si substrate capped with a 300-nm-thick SiO_2 layer. Optical microscopy[19] and Raman spectroscopy[20] were used to locate the flake and confirm that it was a monolayer. Five Ti/Au 10/50 nm contacts were patterned using standard electron beam lithography and lift-off processing. The GNR is structured to submicron dimensions by another lithography stage and an O_2 plasma etching process. An atomic force micrograph of the final device is shown in Fig. 1(a). The GNR is ≈90-nm wide and ≈800-nm long, and the inline QD is ≈200 nm in diameter D.

Figure 1(b) shows the conductance G as a function of the voltage V_{BG} applied to the Si back gate at a temperature of $T =$ 100 mK. The overall form of $G(V_{BG})$ has the V shape expected for graphene, but with a region of suppressed conductance around the charge neutrality point (CNP) characteristic of GNRs at low temperature.[2,3] The fact that the CNP is close to $V_{BG} = 0$ V suggests that there is little net charged-impurity doping of either carrier type, although the transport gap $\Delta V_{BG} \approx 4$ V reflects the presence of large disorder potential fluctuations.[5,21] Indeed, within the transport gap there are many irregularly spaced peaks in conductance due to the alignment of energy levels in disorder-induced localized states along the GNR. The energy scale of the disorder in our device can be estimated from the corresponding range of Fermi energy $\Delta E_F \approx \hbar v_F \sqrt{2(\alpha/|e|)}$, where α is the back-gate capacitance per unit area, and $v_F = 10^6$ ms^{-1} is the Fermi velocity.[22] This

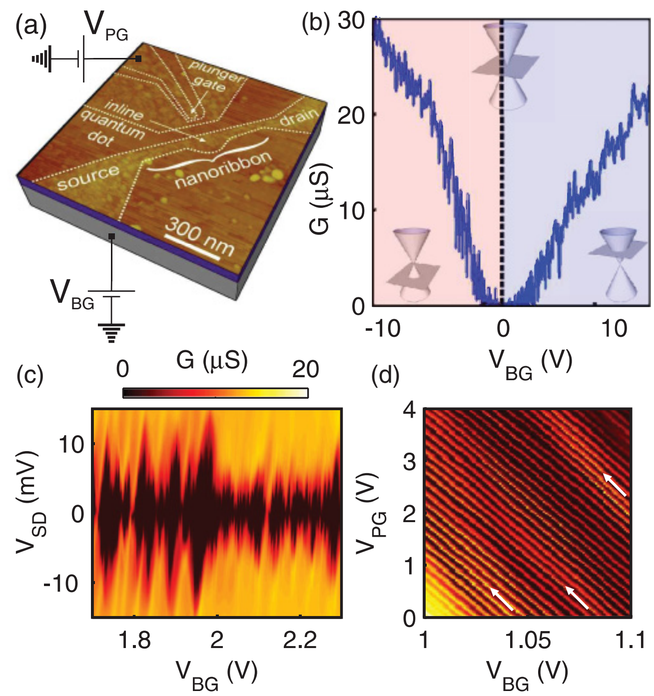

FIG. 1. (Color online) (a) Atomic force micrograph of the GNR ($W \approx 90$, $L \approx 800$ nm) with an inline QD of diameter $D \approx 200$ nm. A functioning GNR intervenes between the QD and the plunger gate, but does not play any role in the results of the present work. (b) Conductance through the GNR as a function of back-gate voltage at $T = 100$ mK. The insets show the position of the Fermi level relative to the Dirac cone over each range of back-gate voltage. (c) Logarithmic conductance as a function of source-drain and back-gate voltages. (d) Conductance as a function of plunger- and back-gate voltages obtained during a different cool down of the device. The white arrows indicate broad resonances stemming from localized states within the constriction.

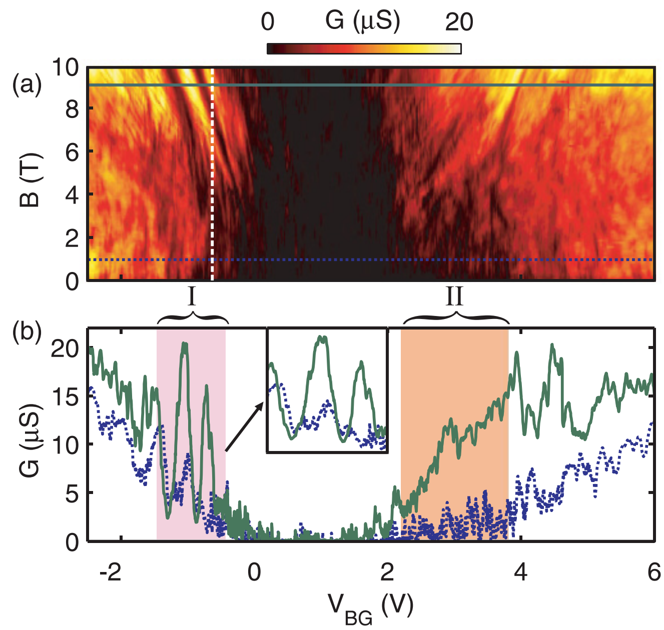

FIG. 2. (Color online) (a) Conductance as a function of back gate and magnetic field. The white dashed line indicates the back-gate voltage used when performing the measurements shown in Fig. 3(a). (b) Line profiles of (a) at 1 (blue, dotted) and 9 T (green, solid). The inset shows a close-up of the highlighted (pink) region I. Highlighted regions show ranges of back-gate voltage where the conductance either oscillates (I) or is uniformly enhanced (II).

yields $\Delta E_F \approx 60$ meV, which is typical for exfoliated GNRs on SiO_2 substrates.[21] The presence of islands is also revealed in Fig. 1(c), which plots G as a function of the source-drain bias V_{SD} and V_{BG}. G is suppressed within diamondlike regions extending $\Delta V_{SD} \approx 4$–15 mV, characteristic of multiple QDs coupled in series.[23] The larger aperiodic diamonds correspond to smaller localized states in the GNR, and the smaller periodic diamonds to the inline QD. The periodic Coulomb blockade (CB) resonances stemming from the inline QD are resolved more clearly in Fig. 1(d), which shows the conductance of the device as a function of back- and plunger-gate voltages. The separation between consecutive peaks is $\Delta V_{PG} \approx 190$ mV and $\Delta V_{BG} \approx 5$ mV. The latter is less than the period $e/C_{BG} \approx 9$ mV expected for a disk with $D = 200$ nm, where $C_{BG} \approx 2\epsilon_0(\epsilon + 1)D \approx 19$ aF and $\epsilon = 4$ for the SiO_2 substrate, probably because the embedded dot extends laterally into the sections of the GNR. To test this idea we use the standard finite-element package COMSOL MULTIPHYSICS to calculate the capacitance of the GNR structure relative to the back and plunger gate. In our model we vary the extent of the central island into the GNR and find good agreement with both the measured capacitances for QD areas of $\approx 0.09\ \mu m^2$, corresponding to a disk with diameter $D \approx 300$ nm. Note that this result is in contrast to previous models where the capacitance of a similar size dot was lower than anticipated theoretically,[24] demonstrating the sensitivity of such estimates to screening effects.

We attribute the broad amplitude modulations of the CB peaks indicated by arrows in Fig. 1(d) to some capacitive coupling between the gates and the localized states in the left and right sections of the GNR, which are well tunnel coupled to the leads and never blockade transport through the QD over this range of V_{BG}. As our plunger gate is located at the center of the GNR, we expect the relative lever arms $\alpha^{\mathrm{GNR}}_{PG/BG}$ of these states to to be similar to one another.[5] Indeed, upon close inspection the only other slope we observe in Fig. 1(d) is $\alpha^{\mathrm{GNR}}_{PG/BG} = 0.0195$, which is slightly smaller than $\alpha^{QD}_{PG/BG} = 0.027$ because of their greater distance from the plunger gate.[5] The larger charging energy of these states, which we estimate to be $\approx$10 meV from the source-drain gap at the apices of the of the larger irregular diamonds in Fig. 1(c), reflects their smaller area.[21]

Figure 2(a) shows $G(V_{BG})$ as a function of magnetic field B. The transport gap shrinks from 4 to 2 V and the conductance on both electron and hole sides increases. The important features in these data are the magnetoconductance oscillations (MCOs) that appear on each side of the transport gap at a relatively low B field ($\approx$5 T) and follow a trajectory intersecting the transport gap as $B \rightarrow 0$ T. Figure 2(b) shows representative cross sections $G(V_{BG})$ through the MCOs at low and high fields. On the hole side (region I), where the MCOs are most pronounced, the MCO minima are comparable to the conductance at a low field [see inset, Fig. 2(b)], while the MCO maxima are of the same size as the regions of uniformly enhanced conductance (region II). The latter fact is a central observation of this work, since it implies the positive magnetoconductance and the MCOs have a common origin. The lower visibility of MCOs on the electron side is probably either related to the degraded mobility, or an effect of the doping from the metallic contacts,[25,26] as suggested by the asymmetry in Fig. 1(b). Note that MCOs with similar behavior were reported previously in side-gated GNRs at a low magnetic field.[3]

To gain further insight into these features in the magnetotransport, we change the QD occupancy using the plunger gate and investigate how the single-particle spectrum evolves while the overall conductance oscillates due to the MCOs. Note that, while single-particle control is also possible using the back gate [see Fig. 1(d)], using the plunger gate simplifies the analysis by maintaining the same carrier density in the large-area graphene leads.[3] Figure 3(a) shows $G(V_{PG})$ as a function of B at $V_{BG} = -0.38$ V [white (dashed) line, Fig 2(a)]. The MCOs [see plot of $G(B)$ in Fig. 3(a)], which have been divided into four regions of minima and maxima for clarity, are superimposed on the periodic CB resonances from the QD. In order to inspect the evolution of the QD spectrum with B, we subtract a smoothed background and construct $\Delta G(N,B)$ in Fig. 3(b), where N is the (zero B field) occupancy estimated by extrapolating the $\nu = -2$ ridge to $B = 0$ T. The range of V_{PG} is equivalent to changing the occupancy by 10 V/0.19 V $\approx$ 50 holes. As a function of B, the CB resonances fluctuate around an average energy until a critical B field where they shift to a lower energy [see resonances highlighted in Fig. 3(b)]. This behavior is well understood and arises from anticrossings between the single-particle levels.[27–29] At a large particle number there are a large number of such anticrossings, so the resonances exhibit kinks without shifting uniformly in energy. In addition, we observe consecutive resonances sharing the same kink structure [Fig. 3(d)], as expected from the two-fold spin degeneracy at low B.[30] This situation changes when the degeneracy of the lowest Landau level (LL) is sufficient to support all the particles, at which point there are no states with lower energy and the resonances follow the trajectory $E_{LL0}(B)$. The critical field B_c above which condensing states can be tracked continuously should follow the $E_{LL-1}(B)$, which corresponds to filling factor $\nu = -2$ in a monolayer QD. Since $\nu = N_{\max}/(\Phi/\Phi_0)$, the number of electrons accommodated by E_{LL-1} is $N_{\max} = 2\Phi/\Phi_0 = eBA/h$. Equating the experimental value of 31 holes/T to $dB_c/dN_{\max}$ [see red dashed line in Fig. 3(b)] yields $A \approx 0.08$ $\mu\mathrm{m}^2$, approximately equal to a disk of diameter $D = 280$ nm. While this is again larger than the lithographic dimensions of the QD would suggest, it is in good agreement with the size deduced from the capacitances between the QD and the gates. The absolute value of $N_{\max}(B_c)$ determined using the above expression is indicated by the $\nu = -2$ white dashed line in Fig. 3(a) and lies precisely at the ridge between regions 2 and 3 of the MCOs. In addition the $\nu = -6$ state is correlated with the lower transition from regions 3 and 4, strongly suggesting both peaks in the MCOs have a common origin related to integer filling, and thus edge state formation. Indeed, the similarity of our data to recent work[31] exploring the crossover to edge channel conduction in suspended GNRs also implies

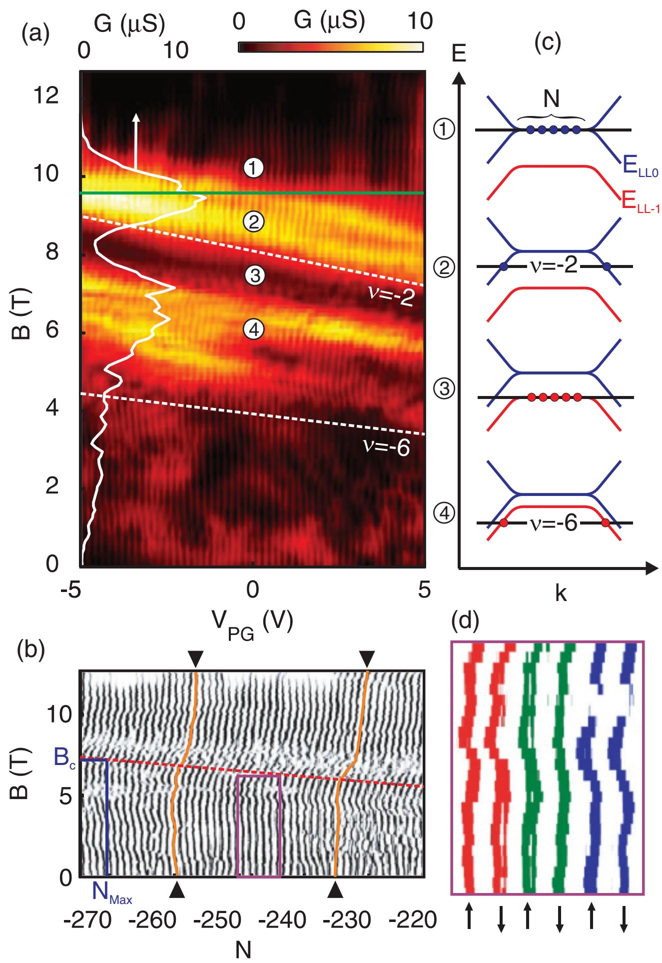

FIG. 3. (Color online) (a) Conductance as a function of plunger-gate voltage and B at $V_{BG} = -0.38$ V [compare with Fig. 2(a)]. Superimposed trace (white, solid) shows the conductance as a function of the magnetic field at $V_{PG} = -5$ V. Green (solid) line indicates fields where line profiles shown in Fig. 4(a) are extracted. (b) Coulomb blockade resonances (black) extracted from the raw $G(V_{PG})$ data in (a) by removing the modulations in the background conductance. Two resonances have been traced over in order to emphasize the shift to a lower energy at a critical field B_c, whose dependence on occupancy follows the red (dashed) line. The relation between B_c and the maximum occupancy $N_{\max}$ of LL_0 has also been indicated. (c) Schematic band structure of a graphene bilayer with zig-zag edges at different magnetic fields. Numbers next to diagram correspond to the regions indicated in (a). The position of the Fermi level in each case is indicated by the black line. (d) Close-up of the region outlined by the purple box in (b) showing three illustrative pairs of resonances sharing the same kink structure, with the implied spin filling sequence shown below.

that the MCOs stem from embryonic edge states, which only suffer from partial backscattering due to the higher disorder in our GNR.

To understand these observations we refer to the LL band-structure schematics of a graphene monolayer at different B shown in Fig. 3(c). In region 1, all states are fully condensed within the flat LL_0. As a consequence the Fermi level is pinned to localized states and the conductance of the GNR is strongly suppressed, consistent with the interaction-induced insulating

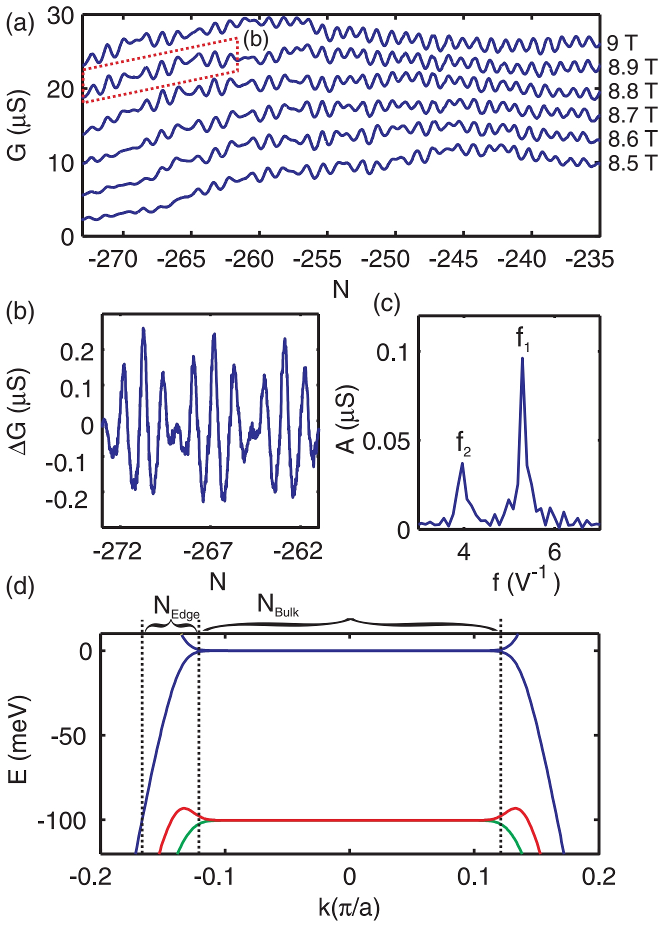

FIG. 4. (Color online) (a) Line sections showing the conductance as a function of estimated occupancy at B between 8.5 and 9 T, in the vicinity of the green (solid) line in Fig. 3(a). (b) High resolution plot of the conductance trace shown in (a) at 8.9 T with a background removed by subtracting a smoothed background. (c) Fourier spectrum of data shown in (b). (d) Tight binding band structure of LL_0 (blue) and LL_{-1} (red/green) of a 1221-atom-wide (150-nm) armchair GNR in a field of 10 T.

behavior observed at high magnetic fields[32] and in suspended GNRs.[31] In region 2, the Fermi level is between LL_0 and LL_{-1}, and the background conductance increases. Within a single particle description, such a correlation between the MCO peak and the elevated conduction *between* CB peaks implies that the tunnel coupling between the single-particle states and the rest of the device is enhanced, as expected for high-mobility chiral edge currents.[17,33] We infer from this that 40–50 holes reside in edge states, which is ≈20% of the total number of degenerate states in LL_0. This process is repeated in regions 3 and 4, although with a much higher ratio of edge to bulk states, possibly due to transmission through uncondensed states belonging to other LLs.[33]

Additional detail relating to the formation of edge states is revealed by the presence of amplitude modulations of the CB peaks. Figure 4(a) shows raw line plots of $G(N)$ at the transition between regions 2 and 3. A periodic "beating" of the CB amplitude appears as the average G starts to decrease in region 2. This is clearer in Fig. 4(b), which shows $\Delta G(N)$ of the raw line profile at 8.9 T in Fig. 4(a). To extract the beat period we inspect the Fourier components of $\Delta G(V_{PG})$ [Fig. 4(c)]. The dominant spectral component $f_1 = 5.291$ V^{-1} corresponds to the CB period. An additional component at $f_2 = 3.968$ V^{-1} emerges in region 2. This corresponds to a beat period $\Delta V_{LL} = 1/(f_2 - f_1) = 0.7559$ V, which envelopes four CB peaks ($\Delta V_{LL}/\Delta V_{PG} = 4$). Such periodic modulations of the CB have been observed in GaAs-based quantum dots, where they arise from cyclic depopulation of LLs together with exclusive coupling to edge states belonging to the lowest LL.[34,35] Since the number of CB peaks per beat period is equal to the number of LLs in the dot,[35] for this mechanism to explain the fourfold beating in region 2 there would need to be a broken fourfold degeneracy in the hole branch belonging to edge states of LL_0. To test this possibility and obtain a semiquantitative analysis of the data, we perform tight-binding simulations to calculate the energy bands of a monolayer armchair GNR in a magnetic field.[36] In order to make our results applicable to the inline quantum dot, we model a GNR whose width W maintains the ratio of the areas occupied by edge and bulk states, $r = A_{\mathrm{edge}}/A_{\mathrm{bulk}} = 4\lambda(D-\lambda)/D^2$. Although the width λ of the edge state region depends on the magnetic field, at $B = 10$ T we find $\lambda \approx 20$ nm and choose $W \approx 150$ nm, i.e., a 1221-atom-wide ribbon. Our results for the wave-vector dependence of LL_0 and LL_{-1} at a $B = 10$ T are shown in Fig. 4(d). The key feature of the simulations which support our interpretation is the ratio of bulk to edge states, (≈17%), which is of the same order as that determined experimentally. To evaluate this ratio we considered the states in the range [−1,1] meV for the bulk, and the states within −1 meV and the onset of the highest LL_{-1} band for the (hole) edge states [Fig. 4(d)].

It is clear from our simulations, however, that the broken valley degeneracy of the edge states belonging to $\nu = 0$ produces only one spin degenerate hole edge state. Combined with Zeeman splitting,[30] this would lead to two edge states whose spatial separation would result in a modified tunnel coupling to the rest of the GNR and a corresponding twofold beating in the amplitude of the CB peaks. The failure of the single-particle picture to explain the fourfold beating points to the need to consider charge redistributions due to Coulomb interaction effects within the many-body $\nu = 0$ ground state,[37] dispersion in the energy of edge channels of adjacent QDs due to inhomogeneous doping,[38] and deviations from the ↑↓↑↓ spin filling sequence.[30]

In conclusion, we have shown how an inline quantum dot can be used to probe the positive magnetoconductance and formation of edge states in graphene nanoribbon structures. The dominant effect of embedding the quantum dot is the appearance of pronounced magnetoconductance oscillations at the edge of the transport gap. By inspecting how the single-particle spectrum evolves in the presence of these oscillations, we deduced that the enhanced conductance arises around an integer filling factor when the states converge to the lowest Landau level. We found a fourfold beating of the Coulomb blockade transmission amplitude during edge state conduction, which we attribute to the influence of inhomogeneities and interaction-induced properties not included in the single-particle picture of the quantum Hall regime. We speculate that the process of edge state formation, when it occurs within the multiple localized states along the GNR, is responsible for the overall positive magnetoconductance and shrinking of the transport gap observed in GNRs. The demonstrated sensitivity of magnetic edge channels to potential disorder also provides a tool for probing the electronic properties of GNRs created by various lithographic techniques.

This work was financially supported by the European GRAND project (ICT/FET, Contract No. 215752) and EPSRC. A.C.F. acknowledges ERC Grant NANOPOTS, EU Grants RODIN and GENIUS, a Royal Society Wolfson Research Merit Award, and EPSRC Grants No. EP/GO30480/1 and No. EP/GO42357/1. A.C. acknowledges the support of Fondation Nanosciences via the RTRA Dispograph project.

[1] Z. Chen, Y.-M. Lin, M. J. Rooks, and P. Avouris, Physica E **40**, 228 (2007).
[2] M. Y. Han, B. Özyilmaz, Y. Zhang, and P. Kim, Phys. Rev. Lett. **98**, 206805 (2007).
[3] F. Molitor, A. Jacobsen, C. Stampfer, J. Güttinger, T. Ihn, and K. Ensslin, Phys. Rev. B **79**, 075426 (2009).
[4] K. Todd, H.-T. Chou, S. Amasha, and D. Goldhaber-Gordon, Nano Lett. **9**, 416 (2009).
[5] C. Stampfer, J. Güttinger, S. Hellmuller, F. Molitor, K. Ensslin, and T. Ihn, Phys. Rev. Lett. **102**, 056403 (2009).
[6] X. Liu, J. B. Oostinga, A. F. Morpurgo, and L. M. K. Vandersypen, Phys. Rev. B **80**, 121407 (2009).
[7] P. Gallagher, K. Todd, and D. Goldhaber-Gordon, Phys. Rev. B **81**, 115409 (2010).
[8] B. Terrés, J. Dauber, C. Volk, S. Trellenkamp, U. Wichmann, and C. Stampfer, Appl. Phys. Lett. **98**, 032109 (2011).
[9] F. Sols, F. Guinea, and A. H. Castro Neto, Phys. Rev. Lett. **99**, 166803 (2007).
[10] M. Y. Han, J. C. Brant, and P. Kim, Phys. Rev. Lett. **104**, 056801 (2010).
[11] M. R. Connolly, K. L. Chiu, A. Lombardo, A. Fasoli, A. C. Ferrari, D. Anderson, G. A. C. Jones, and C. G. Smith, Phys. Rev. B **83**, 115441 (2011).
[12] S. Dröscher, H. Knowles, Y. Meir, K. Ensslin, and T. Ihn, Phys. Rev. B **84**, 073405 (2011).
[13] J. Bai, R. Cheng, F. Xiu, L. Liao, M. Wang, A. Shailos, K. L. Wang, Y. Huang, and X. Duan, Nat. Nanotechnol. **5**, 655 (2010).
[14] J. B. Oostinga, B. Sacépé, M. F. Craciun, and A. F. Morpurgo, Phys. Rev. B **81**, 193408 (2010).
[15] B. I. Shklovskii and A. L. Efros, *Electronic Properties of Doped Semiconductors* (Springer-Verlag, Berlin, 1984).
[16] M. E. Gershenson, Y. B. Khavin, A. G. Mikhalchuk, H. M. Bozler, and A. L. Bogdanov, Phys. Rev. Lett. **79**, 725 (1997).
[17] J.-M. Poumirol, A. Cresti, S. Roche, W. Escoffier, M. Goiran, X. Wang, X. Li, H. Dai, and B. Raquet, Phys. Rev. B **82**, 041413(R) (2010).
[18] R. Ribeiro, J. M. Poumirol, A. Cresti, W. Escoffier, M. Goiran, J.-M. Broto, S. Roche, and B. Raquet, Phys. Rev. Lett. **107**, 086601 (2011).
[19] C. Casiraghi, A. Hartschuh, E. Lidorikis, H. Qian, H. Harutyunyan, T. Gokus, K. S. Novoselov, and A. C. Ferrari, Nano Lett. **7**, 2711 (2007).
[20] A. C. Ferrari, J. C. Meyer, V. Scardaci, C. Casiraghi, M. Lazzeri, F. Mauri, S. Piscanec, D. Jiang, K. Novoselov, S. Roth *et al.*, Phys. Rev. Lett. **97**, 187401 (2006).
[21] F. Molitor, C. Stampfer, J. Güttinger, A. Jacobsen, T. Ihn, and K. Ensslin, Semicond. Sci. Technol. **25**, 034002 (2010).
[22] K. S. Novoselov, A. K. Geim, S. V. Morozov, D. Jiang, Y. Zhang, S. V. Dubonos, I. V. Grigorieva, and A. A. Firsov, Science **306**, 666 (2004).
[23] I. M. Ruzin, V. Chandrasekhar, E. I. Levin, and L. I. Glazman, Phys. Rev. B **45**, 13469 (1992).
[24] L. A. Ponomarenko, F. Schedin, M. I. Katsnelson, R. Yang, E. W. Hill, K. S. Novoselov, and A. K. Geim, Science **320**, 356 (2008).
[25] B. Huard, N. Stander, J. A. Sulpizio, and D. Goldhaber-Gordon, Phys. Rev. B **78**, 121402 (2008).
[26] T. Mueller, F. Xia, M. Freitag, J. Tsang, and P. Avouris, Phys. Rev. B **79**, 245430 (2009).
[27] J. Güttinger, C. Stampfer, F. Libisch, T. Frey, J. Burgdörfer, T. Ihn, and K. Ensslin, Phys. Rev. Lett. **103**, 046810 (2009).
[28] S. Schnez, K. Ensslin, M. Sigrist, and T. Ihn, Phys. Rev. B **78**, 195427 (2008).
[29] F. Libisch, S. Rotter, J. Güttinger, C. Stampfer, and J. Burgdorfer, Phys. Rev. B **81**, 245411 (2010).
[30] J. Güttinger, T. Frey, C. Stampfer, T. Ihn, and K. Ensslin, Phys. Rev. Lett. **105**, 116801 (2010).
[31] Dong-Keun Ki and Alberto F. Morpurgo, arXiv:1203.0540v1 [cond-mat.mes-hall] (unpublished).
[32] J. G. Checkelsky, L. Li, and N. P. Ong, Phys. Rev. B **79**, 115434 (2009).
[33] T. Heinzel, A. T. Johnson, D. A. Wharam, J. P. Kotthaus, G. Böhm, W. Klein, G. Tränkle, and G. Weimann, Phys. Rev. B **52**, 16638 (1995).
[34] P. L. McEuen, E. B. Foxman, U. Meirav, M. A. Kastner, Y. Meir, N. S. Wingreen, and S. J. Wind, Phys. Rev. Lett. **66**, 1926 (1991).
[35] A. A. M. Staring, B. W. Alphenaar, H. van Houten, L. W. Molenkamp, O. J. A. Buyk, M. A. A. Mabesoone, and C. T. Foxon, Phys. Rev. B **46**, 12869 (1992).
[36] P. Gava, M. Lazzeri, A. M. Saitta, and F. Mauri, Phys. Rev. B **79**, 165431 (2009).
[37] T. H. Oosterkamp, J. W. Janssen, L. P. Kouwenhoven, D. G. Austing, T. Honda, and S. Tarucha, Phys. Rev. Lett. **82**, 2931 (1999).
[38] A. Cresti (unpublished).